



# Solvent influence on excited-state intramolecular proton transfer in 3-hydroxychromone derivatives studied by cryogenic high-resolution fluorescence spectroscopy

Arjen N. Bader<sup>a</sup>, Vasyly Pivovarenko<sup>b</sup>, Alexander P. Demchenko<sup>c</sup>,  
Freek Ariese<sup>a</sup>, Cees Gooijer<sup>a,\*</sup>

<sup>a</sup> Department of Analytical Chemistry and Applied Spectroscopy, Laser Centre, Vrije Universiteit, De Boelelaan 1083, 1081 HV Amsterdam, The Netherlands

<sup>b</sup> Department of Chemistry, Kiev Taras Shevchenko University, Kiev 01033, Ukraine

<sup>c</sup> TUBITAK Research Institute for Genetic Engineering and Biotechnology, Gebze-Kocaeli 41470, Turkey

Received 3 June 2002; received in revised form 16 October 2002; accepted 16 October 2002

## Abstract

High-resolution Shpol'skii spectra (recorded at 10 K in *n*-octane) of 3-hydroxychromone (3HC) substituted at the 2-position with a furan (3HC-F), a benzofuran (3HC-BF) or a naphthofuran group (3HC-NF) are presented. Being close analogues of 3-hydroxyflavone (3HF), these compounds can undergo excited-state intramolecular proton transfer (ESIPT). Luminescence can occur from the normal N\* state (blue) or from the tautomeric T\* state (green). Whether blue or green emission is observed is strongly dependent on hydrogen-bonding interactions with the environment. For all three chromones studied, high-resolution emission spectra in the green region (T\* → T) were obtained in pure *n*-octane, showing four sites with distinct emission bands and detailed vibrational structures, whereas no blue emission was detected. Contrary to the spectra published for 3HF, the emission lines were very narrow (line-broadening effects beyond detection) which implies that the ESIPT rate constants are  $> 10^{12} \text{ s}^{-1}$ , at least 25 times lower than for 3HF. In order to study the effects of hydrogen-bonding solvents, four isomers of octanol (1-, 2-, 3- and 4-octanol) were added, forming 1:1 complexes with the 3HC derivatives. For all the combinations considered both blue and additional green emission was observed and in some cases narrow-banded spectra were obtained, mostly in the green. Only for the 3HC-NF/2-octanol complex, narrow-banded emission was found both in the blue and in the green region. It is demonstrated that these emissions come from different configurations of the complex. Possible structures for the two complex species are proposed, supported by semi-empirical calculations on complex formation enthalpies.

© 2002 Elsevier Science B.V. All rights reserved.

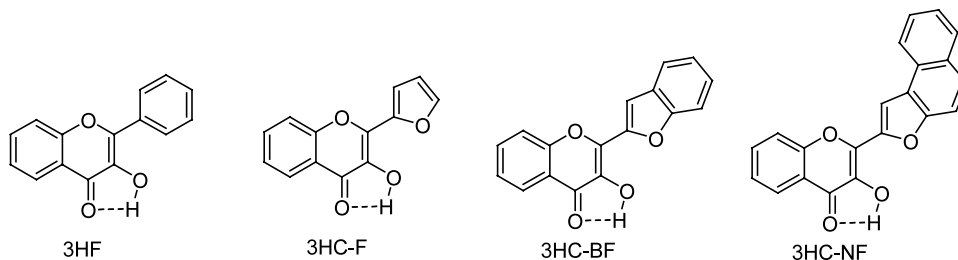
**Keywords:** Chromone derivatives; 3-Hydroxyflavone; Shpol'skii spectroscopy; ESIPT; Proton transfer; Ratiometric probe

## 1. Introduction

\* Corresponding author. Tel.: +31-20-444-7540; fax: +31-20-444-7543.

E-mail address: [gooijer@chem.vu.nl](mailto:gooijer@chem.vu.nl) (C. Gooijer).

For more than 20 years it has been known that 3-hydroxyflavone (3HF, see [Scheme 1](#)) undergoes



Scheme 1. Chemical structures of 3HF, 3HC-F, 3HC-BF, and 3HC-NF.

excited-state intramolecular proton transfer (ESIPT) [1]. The interesting feature of this molecule is that fluorescence can be observed originating from two different excited states, its normal form ( $N^*$ ) and its tautomeric form ( $T^*$ ). Numerous experiments have demonstrated that, in solution, the occurrence of these emissive forms depends on both non-specific interactions with the solvent (polarity effects) and on competition from hydrogen-bonding solvent molecules for the intramolecular hydrogen bond between the 3-hydroxy group and the 4-carbonyl, which is the site of the ESIPT reaction [2–7]. In the presence of a hydrogen-bonding solvent, mainly blue emission (380–460 nm) originating from  $N^*$  is observed. In a non-polar solvent, however, ESIPT takes place and the tautomer  $T^*$  is formed that emits in green (510–570 nm). Various methods, including fluorescence lifetime measurements [2–7], matrix isolation in argon [8,9] and ultrafast pump/probe experiments [10–12] have been used to determine the rate of the transfer process and to study the transfer mechanism both in the presence and absence of a hydrogen-bonding solvent.

The application in these studies of high-resolution spectroscopy in cryogenic Shpol'skii matrices is very attractive, since it allows one to exclude the universal solute–solvent interactions that generate the inhomogeneous broadening of spectra and produce solvent polarity effects that may influence the ESIPT kinetics. In a recent paper [13], we showed that detailed kinetic and mechanistic information about the proton transfer in 3HF can be obtained using steady-state Shpol'skii spectroscopy in *n*-octane at 10 K. When comparing the Shpol'skii excitation and emission spectra of 3HF to those of its deuterated analogue 3-

deuterioxyflavone (3DF), the bandwidths observed for the latter were much narrower. The reason for this is that deuteron transfer is much slower than proton transfer; apparently for 3HF the additional (homogeneous) broadening is due to lifetime effects, whereas for 3DF such effects are rather small. Since the lifetime of  $N^*$  is limited by ESIPT, the additional broadening in the excitation spectrum is a measure for the rate of that process. In a similar way, the rate of back proton transfer (BPT) from the tautomeric ground-state  $T$  to the normal ground-state  $N$  can be obtained from the additional broadening in the  $T^* \rightarrow T$  emission spectrum. Thus, it was estimated that ESIPT takes place in  $39 \pm 10$  fs, whereas BPT is five times slower:  $210 \pm 30$  fs. These results are in good agreement with the data obtained in recent ultrafast pump/probe experiments, where an instrument-limited 35 fs was reported for the rise time of  $T^*$  [10]. Furthermore, it should be noted that the results point to a tunnelling mechanism of proton/deuteron transfer that may be coupled with vibrations along the intramolecular hydrogen bond.

In addition, it was shown that the Shpol'skii approach can be used to study the effect of a hydrogen-bonding impurity in detail [13]. It was found that only a few hydrogen-bonding impurities are able to form a complex with 3HF that fits in the *n*-octane matrix and that their geometrical structure is a key factor; only two of the four octanol isomers yielded high-resolution Shpol'skii spectra. It was observed that when a minor amount of 2-octanol was added, an additional site appeared in emission that was about 7 nm blue shifted. Addition of a much larger amount of 3-octanol had a similar effect, whereas addition of 1-octanol or 4-octanol did not change the spectrum

at all. Apparently, the position of the hydroxy group in octanol determines whether or not the 3HF/octanol complex fits in the matrix and gives rise to the narrow-banded structure of the spectrum. The vibrational energies of the additional sites observed in the presence of 2-octanol or 3-octanol were different from the ones of uncomplexed 3HF. It was concluded that the additional sites originate from 3HF/2-octanol (or 3HF/3-octanol) complexes. Both ESIPT and BPT are influenced by the presence of the OH group of octanol and a model for the changed proton transfer mechanism in these complexes was suggested.

As mentioned earlier, 3HF and its derivatives show very intense fluorescence spectra with a large separation between the N\* and T\* emission bands. They are highly sensitive to the polarity and the hydrogen-bonding properties of the environment. Because of these unique features, they are often used as fluorescent probes for micelles, proteins and biological membranes [14–20]. Most important in this respect is their application as two-wavelength ratiometric probes for spectroscopy and microscopy of living cells [14]. Attempts to improve these properties have been made during recent years [14,21–23]. Most successful in this respect was the substitution of the 2-phenyl group by furyl derivatives, which led to an increase in fluorescence quantum yield and lifetime and a shift in both absorption and fluorescence spectra to longer wavelengths. These molecules show increased sensitivity to solvent perturbations. In this paper, we focus on three 2-furyl derivatives, i.e., on 2-furyl-3-hydroxychromone (3HC-F), 2-benzofuryl-3-hydroxychromone (3HC-BF) and 2-naphthofuryl-3-hydroxychromone (3HC-NF; see Scheme 1). The spectroscopic properties of 3HC-BF and 3HC-NF have already been described in previous papers [14,21]. In order to understand their increased sensitivity to solvent perturbations, detailed information about the structures of the complexes between the 3HC derivatives and the hydrogen-bonding molecule is needed. In this paper, steady-state Shpol'skii spectroscopy is used for this purpose. It will be shown that two different types of monosolvate complexes can be formed, one in which the proton transfer is fully

prohibited and one in which the proton transfer is influenced to a minor extent. Furthermore, the most likely structures of these complexes are presented.

## 2. Experimental

The synthesis of 3HC-BF and 3HC-NF has been described in earlier work [21]. Klymchenko (TUBITAK RIGEB, Turkey) kindly provided these samples. 3HC-F was prepared by alkaline condensation of 2-furaldehyde with 2-hydroxyacetophenone (both obtained from Aldrich) and subsequent oxidative heterocyclization of the resulting chalcone with hydrogen peroxide [24]. Light greenish-yellow crystals of 3HC-F were recrystallized twice from ethanol to give a pure product according to TLC and  $^1\text{H}$  NMR with m.p. 171–172 °C. In the mass spectrum, the chromone 3HC-F showed the peak of the molecular ion  $\text{M}^+$  at 228 c.u. (the calculated molecular mass for  $\text{C}_{13}\text{H}_8\text{O}_4$  is 228.2). The  $^1\text{H}$  NMR spectrum of 3HC-F was measured on a Varian Mercury-400 apparatus in  $\text{DMSO}-d_6$ . Below are the chemical shifts, multiplicities (s—singlet, d—doublet, t—triplet, m—multiplet), and signal intensities (in brackets): 9.80s (1H), 8.12d (1H), 7.90s (1H), 7.74t (1H), 7.63d (1H), 7.43t (1H), 7.31d (1H), 6.70m (1H). The  $^{13}\text{C}$  NMR spectrum of 3HC-F was measured in acetone- $d_6$ : 147.7, 136.5, 128.5, 127.6, 121.2, 118.8, 115.7 (all-tertiary carbons), 175.4, 157.9, 147.3, 141.9, 139.4, 124.2 (quaternary carbons).

Semi-empirical theoretical calculations were performed to determine the possible geometrical structures in the electronic ground state and the formation energies of a number of 3HC-F/octanol complexes. Energy minimization in vacuo was done with the semi-empirical AM1 method using the MOPAC 6.0 program.

10  $\mu\text{M}$  solutions of 3HC-F, 3HC-BF or 3HC-NF in puriss *n*-octane (Fluka) were studied. The solvents 1-, 2-, 3- and 4-octanol (all >97% purity) were obtained from Fluka, Sigma, Fluka and Aldrich, respectively. The samples were transferred to a home-made sample holder containing four sample cells. The sample holder was cooled to

10 K by a Cryodyne Model 21 closed-cycle helium refrigerator (CTI Cryogenics, Waltham, MA). The sample was illuminated at an angle of  $30^\circ$  with a XeCl excimer laser (Lambda Physik LPX 110i, Göttingen, Germany) pumping a dye laser (Lambda Physik, LPD 3002). The excimer laser was operated at 10 Hz, producing 10 ns 50 mJ pulses. Using QUI as a dye, a tunable output in the 370–400 nm range was obtained, while Exalite 411 was used to excite in the range from 403 to 420 nm; excitation spectra were recorded with 0.05 nm steps. The fluorescence emission was collected by a 3 cm F/1.2 quartz lens and focused on the entrance slit of a Spex 1877 0.6 m triple monochromator (Edison, NJ) by a 10 cm F/4 quartz lens. The spectral resolution of this monochromator was 0.1 nm. For detection an Andor Technologies (Belfast, Northern Ireland) intensified CCD camera type iStar DH720-25U-03 was used in the gated mode. The gate was opened at the end of the (scattered) laser light pulse.

### 3. Results and discussion

#### 3.1. Site structures

High-resolution Shpol'skii spectra of the tautomeric form of 3HC-F were obtained using *n*-octane as a solvent, the same solvent used for 3HF. In Fig. 1, an excitation-emission plot of 3HC-F in an *n*-octane matrix at 10 K is shown. It can be seen that 3HC-F is present in four sites in the matrix, with  $T^* \rightarrow T$  (0,0) emission transitions at 520.3, 522.3 (probably two overlapping sites), 523.5 and 525.9 nm, respectively. Three of these sites are simultaneously excited at about 373 nm. Only the  $\lambda_{em} = 525.9$  nm site has a distinctly red shifted  $N \rightarrow N^*$  (0,0) excitation transition, i.e., at 381 nm. Despite the relatively large energy difference between the four sites dealt with, their vibrational energies in emission are the same, i.e., unaffected by the differences in surrounding. Also for 3HC-BF, four sites are present in the high-resolution Shpol'skii spectra obtained in *n*-octane (see Fig. 2). The  $T^* \rightarrow T$  (0,0) emission transitions can be found at 534.2, 537.4, 538.9 and 539.7 nm; their vibrational energies are practically identical. For

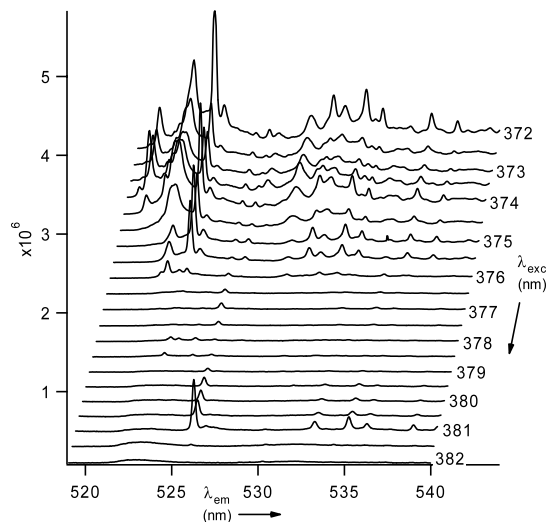


Fig. 1. Emission spectra of 3HC-F in *n*-octane, step-scanning the excitation wavelength from 372 to 382 nm. 3HC-F is present in four sites, emitting at 520.3, 522.3 (probably two overlapping sites), 523.5 and 525.9 nm.

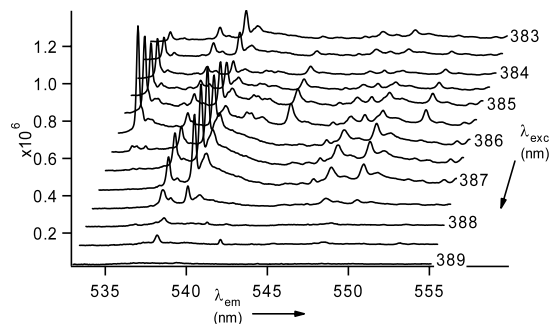


Fig. 2. Emission spectra of 3HC-BF in *n*-octane, step-scanning the excitation wavelength from 383 to 389 nm. 3HC-BF is present in four sites, emitting at 534.2, 537.4, 538.9 and 539.7 nm.

the third compound studied here, i.e., 3HC-NF, high-resolution fluorescence spectra in a 10 K *n*-octane matrix were recorded as well with analogous results. The excitation-emission plot in Fig. 3 shows that 3HC-NF fits in the matrix in four different ways with (0,0) emission transitions at 550.1, 552.9, 555.2 and 558.6 nm, all having similar vibrational energies.

The three compounds studied here have in common that they all fit in an *n*-octane matrix in

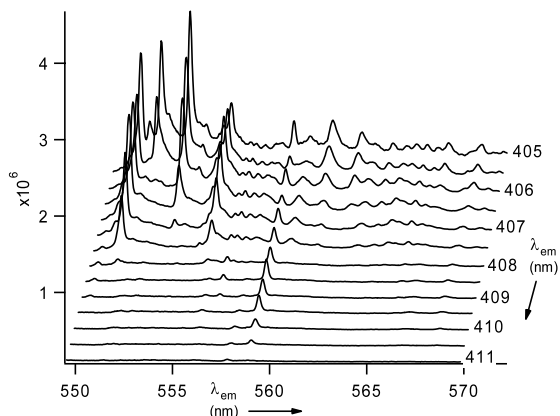


Fig. 3. Emission spectra of 3HC-NF in *n*-octane, step-scanning the excitation wavelength from 405 to 411 nm. 3HC-NF is present in four sites, emitting at 550.1, 552.9, 555.2 and 558.6 nm.

four different ways, whereas 3HF shows only two sites. This difference in site structure can be understood as follows. Probably, the molecule 3HF embedded in the polycrystalline *n*-octane matrix prefers to adopt a planar configuration, although semi-empirical AM1 calculations for this molecule in vacuo indicate that a twisted configuration ( $\phi = 30^\circ$ ) is somewhat more favourable (0.6 kcal/mol) [25]. In the Shpol'skii emission spectrum, two substitutional sites are observed [13] since for the planar 3HF molecule two different orientations are possible in the *n*-octane matrix, a phenomenon quite frequently observed for planar hydrocarbons [26]. Contrary to 3HF, for the three 3HC derivatives concerned the molecule is present in two inequivalent planar conformations, one in which the oxygen of the furan ring is directed towards the oxygen at the 1-position of the chromone ring ( $\phi = 0^\circ$  conformer) and the other in which the oxygen of the furan ring is pointing towards the 3-hydroxy group of the chromone ring ( $\phi = 180^\circ$  conformer). Because these two conformers will have different (0,0) transitions, the total number of sites for 3HC-F increases to 4. Semi-empirical AM1 calculations for the isolated 3HC-F molecule support this interpretation. Contrary to 3HF, for which the  $\phi = 0^\circ$  and  $180^\circ$  conformers are identical; there are indeed two planar conformations, which differ 2.5 kcal/mol in energy. Obviously, these energies may

be different in a crystalline *n*-octane matrix and cannot straightforwardly be used to calculate the intensity distribution over the sites.

### 3.2. Bandwidths

Compared with 3HF, the bandwidths of 3HC-F, 3HC-BF and 3HC-NF in both emission and excitation are very narrow, for the (0,0) line as well as for the vibronic transitions. The bandwidths, obtained from the excitation and emission spectra, are approximately 0.2 nm in all cases. In comparison, for 3HF in excitation, the bandwidth is 10 times larger (2 nm;  $150 \text{ cm}^{-1}$ ) and in emission three to four times larger (0.7 nm;  $26 \text{ cm}^{-1}$ ) [13]. The bandwidths as observed for the 3HC derivatives are amongst the narrowest that can be obtained with our approach. Line-broadening effects in excitation—reflecting the rate of excited-state proton transfer  $\text{N}^* \rightarrow \text{T}^*$ —are, therefore, beyond detection. The same holds for the bandwidth in emission that reflects the BPT from T to N in the electronic ground state. Also here, the proton transfer rates in 3HC-F, 3HC-BF and 3HC-NF appear to be too low to affect the bandwidths. Nonetheless, from the observed widths the maximum values of the ESIPT and BPT rates of furyl derivatives of 3-hydroxychromone can be inferred; they are both lower than  $10^{12} \text{ s}^{-1}$ . This is much slower than ESIPT ( $25 \times 10^{12} \text{ s}^{-1}$ ) and BPT ( $5 \times 10^{12} \text{ s}^{-1}$ ) in 3HF [13]. Apparently, the energy barrier heights and the energy differences between  $\text{N}^*$  and  $\text{T}^*$  for ESIPT and between N and T for BPT are significantly different for both molecules, leading to very different tunnelling rates. Theoretical calculations to support and quantify this interpretation are beyond the scope of the work presented here.

### 3.3. Effects of hydrogen-bonding impurities

As mentioned in Section 1, liquid-state experiments have shown that in comparison to 3HF the 3HC derivatives have an increased sensitivity to solvent effects, but in hydrogen-bonding solvents one cannot distinguish the effects of polarity and of hydrogen-bonding proper. Since in Shpol'skii matrices the inhomogeneous broadening is largely

eliminated, these spectra provide more detailed information and one can study the effects of the furyl moiety on hydrogen bonding under conditions that are not influenced by solvent polarity. This approach was successfully applied in the studies of 3HF [13]. In this study, we have systematically investigated the complexes formed between the 3HC derivatives and a hydrogen-bonding impurity by Shpol'skii spectroscopy. Since the 3HC derivatives considered fit in an *n*-octane matrix, four octanol isomers were used to model the hydrogen-bonding impurity; these solvent molecules have the highest probability of forming a complex that fits in the matrix as well.

We observed that when any of the octanol isomers was added to 3HC-F, 3HC-BF or 3HC-NF, in the low-temperature emission spectra both blue emission of the N\* form and additional green emission of the T\* form could be seen. Interestingly, not all the emission observed was narrow banded. In the case of 3HC-F, only in the presence of 2-octanol did we obtain narrow-banded green emission, coming from an additional site with the (0,0) emission transition at 510.1 nm (see Fig. 4); in the blue emission no sharp lines could be observed. For 3HC-BF, only addition of 2-octanol or (although less favourable) 3-octanol gave rise to

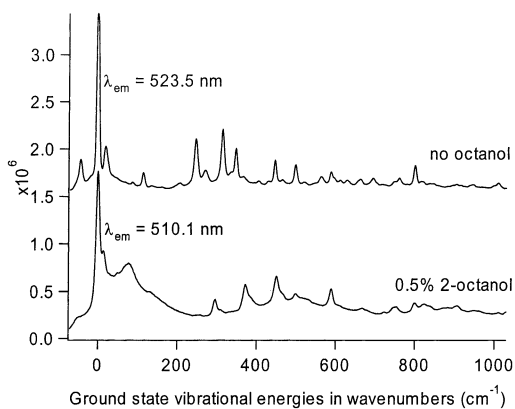


Fig. 4. Shpol'skii emission spectra of 3HC-F in *n*-octane at 10 K. The upper spectrum shows one of the sites in the absence of octanol, the lower spectrum shows the additional site upon addition of 0.5% 2-octanol. For ease of comparison, the spectra are plotted as a function of the energy difference in wavenumbers with respect to the (0,0) transition, giving the ground-state vibrational energies. The wavelengths of the (0,0) transitions are also given.

narrow-banded additional emission in the green (see Fig. 5) and also here not in the blue. The (0,0) emission transitions of the 3HC-BF/2-octanol and 3HC-BF/3-octanol complexes were found at 522.2 and 526.4 nm, respectively. It should be emphasized that narrow bands in the blue region were observed for 3HC-NF with 1-octanol or 2-octanol added. The same molecule showed narrow-banded green emission as well, i.e., upon addition of 2-octanol or 3-octanol (see Fig. 6). The associated sites have (0,0) emission transitions at 424.7 (1-octanol added), 416.5, 535.0 (2-octanol added) and 544.3 nm (3-octanol added).

From the results shown here, the following can be concluded. Considering the vibrational patterns of the additional green sites, it should be noted that these are different from the ones of the uncomplexed compounds. This indicates that for the complexed and the uncomplexed molecules the tautomeric species formed are different. Of course,

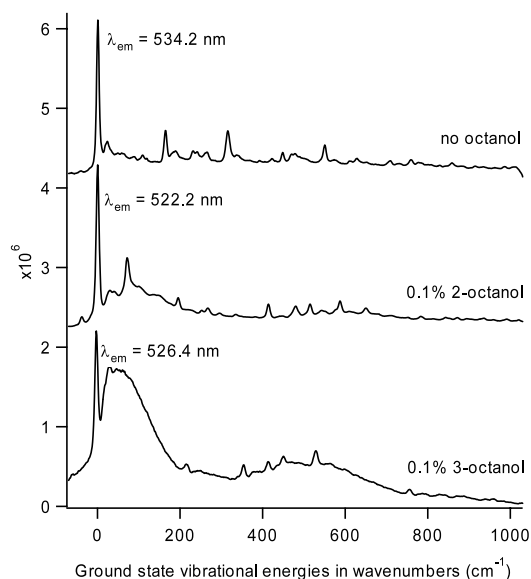


Fig. 5. Shpol'skii emission spectra of 3HC-BF in *n*-octane at 10 K. The upper spectrum shows one of the sites in the absence of octanol, the middle spectrum shows the additional site when 0.1% 2-octanol was added and the lower spectrum shows the additional site in the presence of 0.1% 3-octanol. For ease of comparison, the spectra are plotted as a function of the energy difference in wavenumbers with respect to the (0,0) transition, giving the ground-state vibrational energies. The wavelengths of the (0,0) transitions are also given.

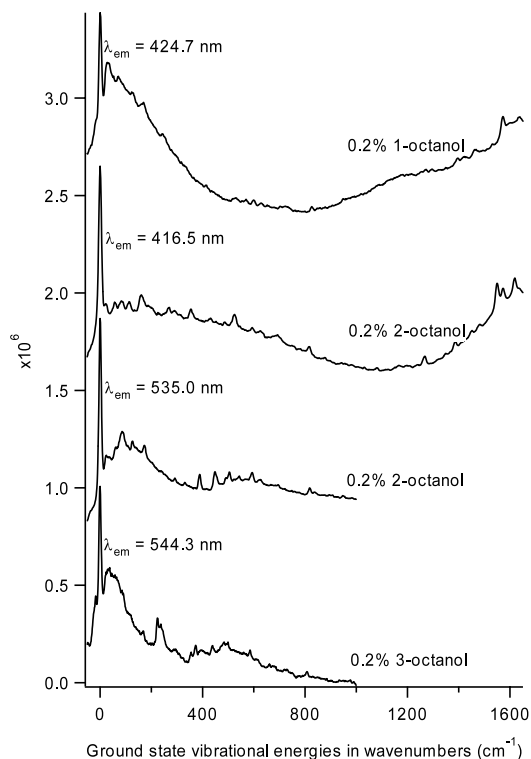


Fig. 6. Shpol'skii emission spectra of 3HC-NF in *n*-octane at 10 K. The upper spectrum shows the blue emission when 0.2% of 1-octanol is added, the second spectrum shows the blue emission upon addition of 0.2% of 2-octanol, the third spectrum shows the additional green site when 0.2% 2-octanol is added and the lower spectrum shows the additional green site in the presence of 0.2% 3-octanol. For ease of comparison, the spectra are plotted as a function of the energy difference in wavenumbers with respect to the (0,0) transition, giving the ground-state vibrational energies. The wavelengths of the (0,0) transitions are also given.

for 3HC-NF, the high-resolution emission spectrum in the blue reflects the ground-state vibrations of the N-form of 3HC-NF in a complex with 1-octanol or 2-octanol. Unfortunately, the vibrational bands in the presence of 1-octanol are very low in intensity; nonetheless they appear to be rather similar to those for the 2-octanol complex. We only obtained more than marginal differences in vibrational energies for the bands at 815/825, 1460/1486, 1550/1570 and 1619/1637  $\text{cm}^{-1}$  for the N-form of 3HC-NF complexed to 1-octanol and 2-octanol (see Fig. 6).

The most striking feature of the results obtained here is the simultaneous presence of both additional green and blue emission upon addition of a hydrogen-bonding impurity, which indicates the emission of both N\* and T\* forms. In principle, this could be explained in two ways. Either the rate of ESIPT is slowed down so heavily that it becomes of the same order of magnitude as the fluorescence decay rate of N\*, i.e., with a factor as large as  $10^3$ – $10^4$ , or, alternatively, two different complex species are observed that behave quite differently as far as ESIPT is concerned. In one of these complexes the proton transfer is influenced, but nonetheless it must be much faster than about  $10^{10} \text{ s}^{-1}$  so that blue emission is obstructed and green emission is observed exclusively. In the other complex, the proton transfer is fully prohibited, i.e., slower than  $10^9 \text{ s}^{-1}$  so that blue emission of N\* is observed and T\* is not formed at all.

If the former explanations were correct, both the blue and the green emission would originate from the same conformation of the 3HC-NF/octanol complex, i.e., from a single species. If such a complex fits in the matrix, then narrow bands are expected both in the blue and in the green. However, from the results shown above it is clear that the presence of narrow bands in the green region does not necessarily mean that the blue emission is narrow banded as well. Therefore, the latter explanation is more likely: the complexes that give emission in the blue are different from the ones that give green emission. Special attention should be given to the case of 3HF-NF in the presence of 2-octanol that showed both narrow-banded blue and green emission (see Fig. 6). In Fig. 7, the Shpol'skii excitation spectra recorded at  $\lambda_{\text{em}} = 445.3$  and 535.0 nm are compared. Because both the band positions and the shapes of these spectra are different, we can conclude that the blue and the additional green fluorescence are emitted from two different complexes indeed.

When considering the possible structures of the “blue” and the “green” complexes, the following has to be taken into account. The complexes are observed at a similar concentration of octanol and show a similar intensity of emission. Furthermore, since a complex composed of more than one solvent molecule is not likely to fit in the matrix

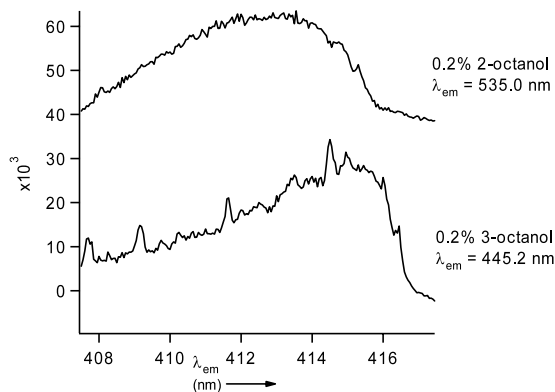


Fig. 7. Shpol'skii excitation spectra of 3HC-NF in *n*-octane upon addition of 0.2% of 2-octanol. The spectrum was obtained by scanning the dye laser and recording a spectrum every 0.05 nm. The upper spectrum shows the excitation spectrum of the additional green site at  $\lambda_{em} = 535.0$  nm. The lower spectrum shows the excitation spectrum of the blue emission at  $\lambda_{em} = 445.2$  (the vibrational band at  $1570\text{ cm}^{-1}$  was chosen as emission wavelength to be able to excite in the (0,0) region as well).

in a regular way, only 1:1 complexes composed of one 3HC derivative and one octanol molecule need to be considered. For the “green” 1:1 complexes, ESIPT takes place while the interaction with the octanol induces a change of the T-ground-state vibrational pattern. For the “blue” 1:1 complexes, the internal hydrogen bond between the carbonyl- and the hydroxy-group is probably weakened or even broken so that ESIPT is inhibited. Finally, the complexes considered should be stable in the N-form of the electronic ground state, otherwise they would not have been formed in the *n*-octane matrix at all. Of course, they should also fit in the matrix in order to show Shpol'skii spectra; unfortunately, this property cannot be easily related to the detailed molecular structure of the complex.

Possible structures for the “green” complexes are given in configurations 1–5 of Table 1. Enthalpies of formation based on minimization in vacuum for the suggested complexes are included in the table. 3HC-F/methanol complexes were used as model systems, because their enthalpies of formation have the same dependence on the structure as 3HC-F/octanol complexes, whereas the calculations for 3HC-F/octanol are less precise than for 3HC-F/methanol because the latter has

fewer degrees of freedom. According to the calculations, the binding of a methanol molecule causes a red shift (1–4 nm) of the absorption maximum in all cases. This is in line with the experimental results.

In the first possible structure, configuration 1 in Table 1, there is a hydrogen bond between the hydrogen of octanol and the oxygen of the chromone's 3-hydroxy group, while in configuration 2 the oxygen of the carbonyl group of the chromone is involved. It is very unlikely that one of these two structures gives the extra green spectra observed because the vibrational pattern of configurations 1 and 2 are not expected to be different from that of uncomplexed 3HC-F. A structure in which—instead of ESIPT—the proton is transferred externally to the hydroxy group of octanol (configuration 3 in Table 1) is unlikely as well: the anion thus created will certainly not emit fluorescence in the narrow green region concerned. The hydrogen bond between the octanol's hydrogen and the oxygen at the 1-position in the chromone ring (configuration 4) is presumably weak so that this structure should also be left out of consideration. This holds even more for the  $S_1$  state where the lone pair electrons of the chromone's oxygen are involved in the  $\pi$ -electronic system that makes it less basic, contrary to the oxygen of the chromone's carbonyl group. The hydrogen bond to the latter group is, therefore, expected to be much stronger, especially in the  $S_1$  state, where charge transfer from the furan to the chromone ring takes place. The most likely structure is, therefore, configuration 5 in Table 1. It is characterized by two hydrogen bonds in which the octanol's hydrogen as well as the octanol's oxygen atoms are involved. For this seven-ring complex, the vibrational energies are expected to be different from those of free 3HC-F. Interestingly, configuration 5 has the most favourable enthalpy of formation within the series of structures considered this far. Although one has to be careful in using such quantitative gas-phase data, they may serve to support the above conclusion. Last, but not least, it should be recalled that a similar complex has been proposed in the case of 3HF/octanol [13].

Table 1  
Possible configurations of complexes formed between the 3HC derivatives and a hydrogen-bonding impurity

Configuration	$H_f$ (kcal/mole) <sup>a</sup>	Normal form	Tautomeric form
1	-110.9 ( $\phi=0^\circ$ ) -110.0 ( $\phi=180^\circ$ )		
2	-112.5 ( $\phi=0^\circ$ ) -110.1 ( $\phi=180^\circ$ )		
3	(No accurate calculation of $H_f$ possible)		
4	-112.3 ( $\phi=0^\circ$ ) -109.1 ( $\phi=180^\circ$ )		
5	-113.1 ( $\phi=0^\circ$ ) -110.5 ( $\phi=180^\circ$ )		
6	-109.3 ( $\phi=180^\circ$ )		
7	-109.5 ( $\phi=166^\circ$ )		

For simplicity 3HC-F is shown. The drawn structures correspond to the  $0^\circ$  conformer, unless otherwise indicated.<sup>a</sup> Formation enthalpy values were calculated for the 3HC-F/methanol 1:1 complexes.

Possible structures of the “blue” complex in which ESIPT is weakened or even blocked are configurations 6 and 7 in Table 1. In these structures, the orientation of the 3-hydroxy group of the chromone is no longer towards the carbonyl

group. Furthermore, since the furyl chromones are much stronger influenced by the presence of a hydrogen-bonding impurity than 3HF, it is feasible that the oxygen of the furan group plays an important role in the complex formation, and so

the furan chromone is probably present in the  $\phi = 180^\circ$  conformation. If the octanol molecule forms a hydrogen bond with the carbonyl group of the chromone, the 3-hydroxy group of the chromone can form a hydrogen bond with the oxygen of the furan ring (configuration 6). Another possibility is the formation of a hydrogen bond between the octanol and the 3-hydroxy group of the chromone, on the one hand, and the furan oxygen, on the other (see configuration 7). The latter structure is less likely than complex 6 because the seven-ring might cause a non-planarity that will not fit very well in the matrix. Gas-phase AM1 calculations indicate that configuration 7 has the energetically most favourable structure at  $\phi = 166^\circ$ .

#### 4. Conclusions

Rather unexpected, for the three uncomplexed furyl derivatives considered the excitation and emission spectra in Shpol'skii matrices at 10 K are much narrower than in the case of 3HF. This means that both ESIPT and BPT are much slower than for 3HF; the associated rate constants cannot be inferred from the bandwidth effects on the spectra. Detailed theoretical studies have to be performed to explain these differences. Furthermore, Shpol'skii spectroscopy provides detailed insight into the influence of hydrogen bonding on the emission of the compounds. The spectra recorded for the 1:1 complexes formed with octanol isomers show both blue (of the N\* form) and green (of the T\* form) emissions that cannot be attributed to a single species but point to different types of the complex. These two complexes are observed simultaneously, one undergoing fast ESIPT and thus producing green emission whereas in the other complex ESIPT is fully inhibited. Obviously, in the liquid state where inhomogeneous broadened bands are observed in emission and excitation, such a distinction cannot be made. The ability to form different types of hydrogen-bonding complexes with different abilities to exhibit ESIPT is probably a unique property of 3HC–3HF systems. These molecules are specifically susceptible to external hydrogen-bonding perturbations, since in the ground state

there is only a weak intramolecular hydrogen bond, which is part of a five-membered ring [27].

#### References

- [1] P.K. Sengupta, M. Kasha, *Chem. Phys. Lett.* 68 (1979) 382.
- [2] G.J. Woolfe, P.J. Thistlethwaite, *J. Am. Chem. Soc.* 103 (1981) 6919.
- [3] M. Itoh, K. Tokumura, Y. Tanimoto, Y. Okada, H. Takeuchi, K. Obi, I. Tanaka, *J. Am. Chem. Soc.* 103 (1981) 4146.
- [4] A.J.G. Strandjord, P.F. Barbara, *Chem. Phys. Lett.* 98 (1983) 21.
- [5] A.J.G. Strandjord, S.H. Courtney, D.M. Friedrich, P.F. Barbara, *J. Phys. Chem.* 87 (1983) 1125.
- [6] D. McMorro, T.P. Dzugan, T.J. Aartsma, *Chem. Phys. Lett.* 103 (1984) 492.
- [7] A.J.G. Strandjord, P.F. Barbara, *J. Phys. Chem.* 89 (1985) 2355.
- [8] B. Dick, N.P. Ernsting, *J. Phys. Chem.* 91 (1987) 4261.
- [9] G.A. Brucker, D.F. Kelley, *J. Phys. Chem.* 91 (1987) 2856.
- [10] S. Ameer-Beg, S.M. Ormson, R.G. Brown, P. Matousek, M. Towrie, E.T.J. Nibbering, P. Foggi, F.V.R. Neuwahl, *J. Phys. Chem. A* 105 (2001) 3709.
- [11] B.J. Schwarz, L.A. Peteanu, C.B.J. Harris, *J. Phys. Chem.* 96 (1992) 3591.
- [12] A. Muhlford, T. Bultmann, N.P. Ernsting, B. Dick, *Femtosecond Reaction Dynamics*, Royal Netherlands Academy of Arts and Sciences, Amsterdam, 1993, p. 83.
- [13] A.N. Bader, F. Ariese, C. Gooijer, *J. Phys. Chem. A* 106 (2002) 2844.
- [14] A.P. Demchenko, A.S. Klymchenko, V.G. Pivovarenko, S. Ercelen, in: R. Kraayenhof, A.J.W.G. Visser, H.C. Geritsen (Eds.), *Fluorescence Spectroscopy, Imaging and Probes—New Tools in Chemical, Physical and Life Sciences*, Springer Series on Fluorescence Methods and Applications, vol. 2, Springer, Heidelberg, 2002.
- [15] O.P. Bondar, V.G. Pivovarenko, E.S. Rowe, *Biochim. Biophys. Acta* 1369 (1998) 119.
- [16] A. Sytnik, D. Gormin, M. Kasha, *Proc. Natl. Acad. Sci. USA* 91 (1994) 11968.
- [17] J. Guharay, P.K. Sengupta, *Spectrochim. Acta A* 53 (1997) 905.
- [18] S.M. Dennison, J. Guharay, P.K. Sengupta, *Spectrochim. Acta A* 55 (1999) 1127.
- [19] J. Guharay, B. Sengupta, P.K. Sengupta, *Proteins* 43 (2001) 71.
- [20] G. Duportail, A.S. Klymchenko, Y. Mely, A.P. Demchenko, *FEBS Lett.* 508 (2001) 196.
- [21] A.S. Klymchenko, T. Ozturk, V.G. Pivovarenko, A.P. Demchenko, *Can. J. Chem.* 79 (2001) 358.
- [22] S. Ercelen, A.S. Klymchenko, A.P. Demchenko, *Anal. Chim. Acta*, 464 (2002) 273.

- [23] A.S. Klymchenko, T. Ozturk, V.G. Pivovarenko, A.P. Demchenko, *Tetrahedron Lett.* 42 (2001) 7967.
- [24] M.A. Smith, R.M. Neumann, R.A. Webb, *J. Heterocyc. Chem.* 5 (1968) 425.
- [25] A.S. Klymchenko, V.G. Pivovarenko, A.P. Demchenko, *Spectrochim. Acta A*, submitted for publication.
- [26] I. Renge, U.P. Wild, Principles in matrix-induced high-resolution optical spectroscopy and electron–proton coupling in doped organic glasses, in: C. Gooijer, F. Ariese, J.W. Hofstraat (Eds.), *Shpol'skii Spectroscopy and Other Site Selection Methods*, Wiley, New York, 2000.
- [27] D. McMorrow, M. Kasha, *J. Phys. Chem.* 88 (1984) 2235.